The Asp^{272}–Glu^{282} Region of Platelet Glycoprotein Ibα Interacts with the Heparin-binding Site of α-Thrombin and Protects the Enzyme from the Heparin-catalyzed Inhibition by Antithrombin III*

Raimondo De Cristofaro‡§, Erica De Candia‡, Sergio Rutella¶, and Jeffrey I. Weitz‖**

From the ‡Haemostasis Research Center and the ¶Center for the Flow Cytometric Study of Blood Cells, Catholic University School of Medicine, Largo F. Vito, 00168 Rome, Italy and the ‖Hamilton Civic Hospitals Research Centre and McMaster University, Hamilton, Ontario L8V 1C3, Canada

Platelet glycoprotein Ib (GpIb) mediates interaction with both von Willebrand factor and thrombin. Thrombin binds to GpIb via its heparin-binding site (HBS) (De Candia, E., De Cristofaro, R., De Marco, L., Mazzucato, M., Picozzi, M., and Landolfi, R. (1997) *Thromb. Haemostasis* 77, 735–740; De Cristofaro, R., De Candia, E., Croce, G., Morosetti, R., and Landolfi, R. (1998) *Biochem. J.* 332, 643–650). To identify the thrombin-binding domain on GpIbα, we examined the effect of GpIbα$_{1-282}$, a GpIbα fragment released by the cobra venom mocarhagin on the heparin-catalyzed rate of thrombin inhibition by antithrombin III (AT). GpIbα$_{1-282}$ inhibited the reaction in a dose-dependent and competitive fashion. In contrast, the GpIbα$_{1-271}$ fragment, produced by exposing GpIbα$_{1-282}$ to carboxypeptidase Y, had no effect on thrombin inhibition by the heparin-AT complex. Measurements of the apparent equilibrium constant of the GpIbα$_{1-282}$ binding to thrombin as a function of different salts (NaCl and tetramethyl-ammonium chloride) concentration (0.1–0.2 M) indicated a large salt dependence (Γ$_±$ = −4.5), similar to that pertaining to the heparin binding to thrombin. The importance of thrombin HBS in its interaction with GpIbα was confirmed using DNA aptamers, which specifically bind to either HBS (HD22) or the fibrinogen recognition site of thrombin (HD1). HD22, but not HD1, inhibited thrombin binding to GpIbα$_{1-282}$. Furthermore, the proteolytic derivative γ$_T$-thrombin, which lacks the fibrinogen recognition site, binds to GpIbα via its intact HBS in a reaction that is inhibited by HD22. Neither α- nor γ$_T$-thrombin bound to GpIbα$_{1-271}$, suggesting that the Asp^{272}–Glu^{282} region of GpIbα may act as a "heparin-like" ligand for the thrombin HBS, thereby inhibiting heparin binding to thrombin. It was also demonstrated that intact platelets may dose-dependently inhibit the heparin-catalyzed thrombin inhibition by AT at enzyme concentrations <5 nM. Altogether, these findings show that thrombin HBS binds to the region of GpIbα involving the Asp^{272}–Glu^{282} segment, protecting the enzyme from the inactivation by the heparin-AT system.

§ To whom correspondence should be addressed: Centro Ricerche Fisiopatologia dell'Emostasi, Istituto di Semeiotica Medica, Università Cattolica S. Cuore, Largo F. Vito 1, 00168 Roma, Italy. Tel.: 39-6-30154438; Fax: 39-6-35503777; E-mail: rdecristofaro@rm.unicatt.it.

** Recipient of a Career Investigator Award from the Heart and Stroke Foundation of Canada.

Platelet glycoprotein Ib (GpIb),[1] which belongs to the so called "leucine-rich repeat" family of proteins, binds to von Willebrand factor, thus allowing the early adhesion of platelets to exposed subendothelium (1, 2). In addition, GpIb also binds to thrombin with high affinity (1). The inhibition of this interaction causes a reduced thrombin-induced platelet activation through an unclear mechanism (3, 4).

GpIb is a 150-kDa transmembrane glycoprotein and contains a 27-kDa β-subunit connected via a disulfide bond to the α-subunit (5). Glycocalicin, the 140-kDa extracytoplasmic portion of GpIbα that bears the von Willebrand and thrombin-binding sites can be prepared by hydrolyzing GpIbα with endogenous calcium-dependent sulfydryl proteases such as calpain (1).

Previous studies have shown that the GpIbα thrombin-binding site maps to an extensive C-terminal region spanning residues Cys^{209}–Asp^{287} (6). Moreover, recent studies, indicate that thrombin binds to GpIb via its heparin-binding site (HBS) (7, 8).

In this study the structural mapping of GpIbα domain that interacts with the HBS on thrombin was further localized to 272–282 residues using GpIbα$_{1-282}$ and GpIbα$_{1-271}$, fragments released from GpIbα upon exposure to either mocarhagin, a cobra venom extract (9), or mocarhagin plus carboxypeptidase Y. To investigate the consequences of the interaction of thrombin with GpIb, we examined the effect of single-stranded DNA oligonucleotides that bind either to the HBS or the fibrinogen recognition site of thrombin on (*a*) the heparin-catalyzed rate of thrombin inhibition by antithrombin III in the presence of paraformaldehyde-treated platelets or the two GpIbα fragments and (*b*) thrombin-induced platelet aggregation.

EXPERIMENTAL PROCEDURES

Materials—Human α-thrombin was purified and characterized as previously reported (10). High molecular weight heparin (lot HF2025; molecular weight = 16,000) was purchased from Enzyme Research Laboratories Inc. (South Bend, IN). The molecular weight of this heparin fraction was confirmed by subjecting the material to gel filtration using a Bio-Silect SEC 250–5 column (Bio-Rad) fitted to a high performance liquid chromatograph (Perkin-Elmer, series 10) and monitoring the fractions at 205 nm. Purified heparin oligosaccharides of known molecular weights were used to construct the reference curve. Heparin with high affinity for antithrombin was isolated by affinity chromatography using an antithrombin III column (11). Antithrombin III (lot HATIII 540AL) purchased from Enzyme Research Labs migrated as a single band on 4–20% SDS-PAGE gels with an apparent molecular mass of 58 kDa. The antithrombin concentration was calculated spectrophotometrically, using an extinction coefficient E_{280} (1%) = 6.5 (12). The chromo-

genic substrate HD-Phe-Pip-Arg-p-nitroanilide (S2238) was from Chromogenix (Mölndal, Sweden). Sodium acetate, C-terminal (55–65) sulfated, and nonsulfated hirudin fragments (Ac-DFEEIPEEY(SO$_3$H)LQ), dansyl-chloride, a dansyl-L-amino acids kit, ethylammonium chloride, lithium carbonate, methanol, trifluoroacetic acid (spectrophotometric grade), trypsin-immobilized agarose (tosylphenylalanyl chloromethyl ketone-treated), and prostaglandin E$_1$ were from Sigma. Carboxypeptidase Y (excision grade), immobilized on Sepharose CL-4B resin, was purchased from Pierce. Mocarhagin, purified from cobra venom (9), was kindly provided by Dr. Robert K. Andrews (Baker Medical Research Institute, Prahran, Australia).

The two single-stranded DNA oligonucleotides (*a*) 5′-AGTCCGTGG-TAGGGCAGGTTGGGGGTGACT-3′, referred to as HD22, and (*b*) 5′-GGTTGGTGTGGTTGG-3′, referred to as HD1, were synthesized by the Institute for Molecular Biology and Biotechnology at McMaster University (Hamilton, ON, Canada).

Purification of GpIbα$_{1–282}$ Fragment—GpIbα$_{1–282}$ was prepared by mocarhagin treatment of washed platelets using a fast protein liquid chromatography method, as previously reported for glycocalicin purification (7). Briefly, platelets from outdated platelet concentrates (50 units) were washed three times by centrifugation in 10 mM Hepes, 0.135 M NaCl, 3 mM KCl, 0.1% bovine serum albumin, 5 μM prostaglandin E$_1$, pH 7.4. After washing, platelet suspensions were treated with 10 μg/ml mocarhagin for 60 min at 37 °C in the above buffer without bovine serum albumin and containing 1 mM CaCl$_2$. This treatment is reported to cause selective cleavage of the amidic bond between Glu^{282} and Asp^{283} of GpIbα (9). At the end of incubation, the reaction was stopped by addition of 2 mM EDTA, and platelets were precipitated by centrifuging at 800 × *g* for 15 min. The supernatant was chromatographed on a high load Q-Sepharose column (Amersham Pharmacia Biotech) connected to a fast protein liquid chromatography apparatus, and GpIbα$_{1–282}$ was isolated according to previously reported methods for glycocalicin purification, using a gradient of 0–0.6 M NaCl for 60 min (7, 8). The peak eluted at 0.55 M NaCl was collected and further analyzed. SDS-PAGE showed that the purified protein had an apparent molecular mass of 40 kDa under both nonreducing and reducing conditions. Purified GpIbα$_{1–282}$ (5 μg) was electrophoresed on a 4–20% SDS-PAGE gel, transferred to nitrocellulose, blotted, and incubated with 2 μg/ml purified mouse MoAb SZ2 purchased from Immunotech (Instrumentation Laboratory, Milano, Italy). This monoclonal antibody recognizes a region of the N-terminal GpIbα domain and inhibits both von Willebrand and thrombin binding to GpIbα. The GpIbα$_{1–282}$ band was detected with alkaline phosphatase-labeled goat anti-mouse IgG (Sigma-Aldrich). GpIbα$_{1–282}$ concentration was determined spectrophotometrically at 280 nm, using a molar extinction coefficient equal to 33390 (cm^{-1}), as predicted on the basis of the sequence (13), by the method of Pace and co-workers (14).

Treatment of GpIbα$_{1–282}$ with Immobilized Carboxypeptidase Y—Purified GpIbα$_{1–282}$ (at concentrations ranging from 5 to 10 μM) in 0.5 ml of 10 mM phosphate buffer, 0.15 M NaCl, pH 6.5, was incubated with 0.5 ml of immobilized carboxypeptidase Y (~6 units) at 37 °C with gentle stirring. At intervals ranging from 10 to 240 min., 50 μl of supernatant from perchlorate-treated samples (0.3 M) were removed and subjected to amino acid analysis according to the method of Levina and Nazimov (15). Briefly, the solution was dried *in vacuo* at 60 °C and evaporated to dryness twice from 5 μl of water. After addition of 40 mM lithium carbonate buffer, pH 9.5, and dansyl chloride (10-fold excess relative to GpIbα$_{1–282}$) in acetonitrile (3 μl), the mixture was centrifuged at 1000 × *g* for 2 min and kept in darkness for 35 min at 20 °C prior to adding 3 μl of 0.1% ethylammonium chloride. After drying at 60 °C, a mixture of 5.7 M HCl and trifluoroacetic acid (2:1 v/v, 6 μl) was added to the precipitate, and the resulting solution was frozen. After drying twice with methanol, the sample was dissolved in methanol (5–10 μl) and injected onto a Brownlee (Santa Clara, CA) RP 300 octyl analytical column (220 × 4.6 mm) connected to a guard column of the same resin. Elution was carried out with the following eluants: (*a*) 0.1% trifluoroacetic acid in water and (*b*) water:acetonitrile (40:60 v/v) in 0.1% trifluoroacetic acid. The applied gradient was 0–99% B in 90 min and 99% B for 5 min at a flow rate of 1 ml/min. In separate experiments, a reference reverse phase high pressure liquid chromatography chromatogram was obtained by using a standard mixture of dansylated amino acids.

The fragment of GpIbα$_{1–282}$ remaining after a 240-min exposure to carboxypeptidase Y (GpIbα$_{1–271}$ fragment) was gel filtered on a Bio-Rad DG10 column and concentrated using an Amicon Centriprep 3 membrane. Its concentration was determined at 280 nm using a molar extinction coefficient equal to 28920 (cm^{-1}). SDS-PAGE showed that
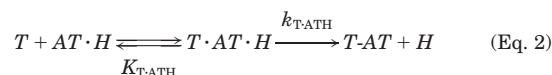
GpIbα$_{1–271}$ did not undergo further intramolecular fragmentation by carboxypeptidase Y.

Because a sulfated tyrosine was expected in the hydrolyzed solution, a reference chromatogram of carboxypeptidase Y-treated (4 h) sulfated and nonsulfated C-terminal hirudin peptide 55–65 (Ac-DFEEIPEEY-(SO$_3$H)LQ) also was obtained. The assignment of the chromatographic peak representing *O*-sulfated L-tyrosine was based on the known amino acid composition of the peptide and the difference in the chromatographic pattern obtained with the sulfated and nonsulfated peptide.

Inactivation of α-Thrombin by Antithrombin III in the Presence and Absence of Heparin and GpIbα$_{1–282}$ Fragment—Previous studies indicated that thrombin interaction with antithrombin (AT) occurs via the following two-step reaction (16, 17).

$$T + AT \rightleftharpoons T \cdot AT \rightarrow T\text{-}AT \qquad (\text{Eq. 1})$$
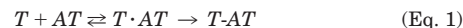
where *T* is thrombin, *T·AT* is the reversible thrombin-antithrombin adduct and *T-AT* is the final complex between enzyme and inhibitor. Heparin accelerates the second step of the reaction by binding to both thrombin and AT (17). Thus, the final T-AT adduct occurs through formation of an intermediary ternary thrombin-heparin-AT complex, which rearranges as follows.

$$T + AT \cdot H \underset{K_{\text{T·ATH}}}{\overset{k_{\text{T·ATH}}}{\rightleftharpoons}} T \cdot AT \cdot H \longrightarrow T\text{-}AT + H \qquad (\text{Eq. 2})$$

where *AT·H* is the reversible antithrombin-heparin complex, *T·AT·H* is the ternary intermediary thrombin-antithrombin-heparin adduct, $K_{\text{T·ATH}}$ is the equilibrium dissociation constant for thrombin binding to the heparin-antithrombin complex, and $k_{\text{T·ATH}}$ is the rate constant for the conversion of the intermediary complex to the final T-AT adduct.

The heparin-catalyzed thrombin-AT interaction can be kinetically analyzed using a formula describing a rapid equilibrium two-substrate enzyme reaction, in which both thrombin and AT are the substrates and heparin is the "enzyme" (17). Under experimental conditions where the thrombin concentration is less than K_m value for the heparin-thrombin interaction and the AT concentration is more than the value for thrombin, one can assume that the inhibitor concentration does not change during the inhibition reaction. This simplifies the mathematical treatment of a two-substrate Michaelis equation, and the rate of thrombin inactivation is well described by the following differential equation.

$$\frac{-dT}{dt} = \frac{k_{\text{cat}}}{K_{\text{T·ATH}}} H_0 \frac{AT_0}{K_{\text{ATH}} + AT_0} T + k_{\text{uncat}} AT_0 T \qquad (\text{Eq. 3})$$

where *T* is thrombin, AT_0 is the AT concentration, H_0 is the heparin concentration, the ratio $k_{\text{cat}}/K_{\text{T·ATH}}$ is the specificity constant for thrombin interaction with heparin under saturating AT concentration, K_{ATH} is the equilibrium dissociation constant for AT-heparin interaction, and k_{uncat} is the second order rate constant for the uncatalyzed thrombin-AT reaction.

Integration of Equation 3 results in the following.

$$T_t = T_0 \exp(-k_{\text{obs}} t) \qquad (\text{Eq. 4})$$

where T_0 and T_t are the thrombin concentrations at time = 0 and time = *t*, respectively. On the basis of Equations 3 and 4 we obtained the following.

$$k_{\text{obs}} = \frac{k_{\text{cat}}}{K_{\text{T·ATH}}} H_0 \frac{AT_0}{K_{\text{ATH}} + AT_0} + k_{\text{uncat}} AT_0 \qquad (\text{Eq. 5})$$

Equation 5 shows that thrombin inactivation is described by a pseudo-first order exponential decay, characterized by a rate constant (k_{obs}) that is linearly correlated with the heparin concentration and hyperbolically plus linearly linked to AT concentration. Thus, the $k_{\text{cat}}/K_{\text{TATH}}$ value can be calculated from the AT dependence of the k_{obs} values, once the K_{ATH} value is known.

In our experimental set-up, k_{obs} was measured by studying inactivation of 1 nM α-thrombin, in the presence of 4 nM heparin, as a function of AT concentration (5–250 nM) in a final volume of 50 μl of 10 mM Tris-HCl, 0.1–0.5 M NaCl, 0.1% PEG 6000, pH 7.50, at 25 °C. Thrombin inhibition by AT was also studied as a function of GpIbα$_{1–282}$ and GpIbα$_{1–271}$ (0–400 nM). At each AT concentration, the reaction was quenched at various intervals by addition of 2 ml of 100 μM Phe-Pip-Arg-pNA in 50 mM Tris-HCl, 0.1 M NaCl, 0.1% PEG 6000, pH 8.00. The k_{obs} value was then calculated using Equation 4.

Because the relationship between the observed $K_{\text{T·ATH}}/k_{\text{cat}}$ values and GpIbα$_{1–282}$ concentration was linear, a competitive scheme was

applied whereby GpIbα$_{1-282}$ binding to thrombin inhibited the binding of heparin to thrombin and *vice versa*. According to this competitive scheme, only the $K_{T\text{-}ATH}$ value is expected to increase as a function of the GpIbα fragment. The experimental values of $K_{T\text{-}ATH}/k_{cat}$ (*i.e.* ($K_{T\text{-}ATH}/k_{cat}$)^{obs}) were thus fitted to the following relation.

$$\left(\frac{K_{T\text{-}ATH}}{k_{cat}}\right)^{obs} = \left(\frac{K_{T\text{-}ATH}}{k_{cat}}\right)^{o}\left(1 + \frac{P}{K_i}\right) \qquad \text{(Eq. 6)}$$

where P is the concentration of GpIbα$_{1-282}$, K_i is the equilibrium binding constant of GpIbα$_{1-282}$ for thrombin, and ($K_{T\text{-}ATH}/k_{cat}$)^{o} is the value of $K_{T\text{-}ATH}/k_{cat}$ for thrombin interaction with the AT-heparin complex in the absence of the GpIbα$_{1-282}$ fragment.

Thrombin inhibition by AT in the absence of heparin was studied using the following reaction scheme for irreversible inhibition (17).

$$T + S \underset{K_m}{\rightleftharpoons} TS \xrightarrow{k_{cat}} T + P \qquad \text{(Eq. 7)}$$
$$+$$
$$AT$$
$$\downarrow k$$
$$T\text{-}AT$$
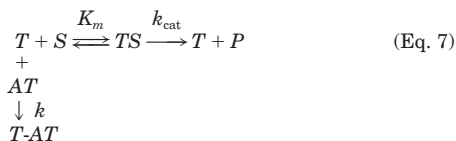
where k is the rate constant for irreversible thrombin inhibition. Experiments were performed by using the Phe-Pip-Arg-pNA substrate and α-thrombin at concentrations of 200 μM and 0.5–3 nM, respectively. Antithrombin was typically used at a concentration of 2.5 μM. The buffer used for these kinetic experiments was 10 mM Hepes, 0.15 M NaCl, 0.1% PEG 6000, pH 7.50, at 25 °C. The concentration of pNA released from the substrate was followed at 405 nm, and the experimental points were fitted to the following equation (17).

$$[\text{pNA}]_t = [\text{pNA}]_{inf}[1 - \exp(kt)] \qquad \text{(Eq. 8)}$$

where $[\text{pNA}]_t$ and $[\text{pNA}]_{inf}$ are the pNA concentration at time = t and time = infinity, respectively, and k is the pseudo-first rate constant for the irreversible thrombin inhibition. The analysis of these data, along with those pertaining to the experiments described above, was performed using GRAFIT software (Erithacus Software Ltd., Staines, UK) based on a modified Marquardt algorithm.

Preparation of γ$_T$-Thrombin—The proteolytic form of thrombin, referred to as γ$_T$-thrombin, was produced using immobilized trypsin, as described previously (18). When subjected to SDS-PAGE under reducing conditions, the purified material showed two bands with a molecular mass of about 26 and 14 kDa, respectively. Purified γ$_T$-thrombin was 100% active, as determined by active site titration with *p*-nitrophenyl-guanidinobenzoate. This thrombin derivative did not clot fibrinogen but was readily inhibited by AT in the presence of heparin, as shown using the assay procedure reported above. Typically, 1 nM γ$_T$-thrombin, 150 nM AT, and 4 nM heparin were used in these inhibition experiments.

Effect of Salt and the Single-stranded DNA Oligonucleotides HD22 and HD1 on Thrombin-GpIbα$_{1-282}$ Interaction—The effect of salt and both HD22 and HD1 on the thrombin-GpIbα 1–282 fragment interaction was studied using a solid phase binding assay. The GpIbα$_{1-282}$ fragment was absorbed to the wells of a Dynatech Immulon microplate by incubating 1 μg/ml GpIb fragment in 0.1 M carbonate buffer, pH 9.60, overnight at 4 °C. The salt dependence of the K_d binding of GpIbα$_{1-282}$ to thrombin was investigated in the salt concentration range from 0.1 to 0.2 M, when NaCl or tetramethylammonium chloride (TMACl) were used, or at 0.2 M, when NaF was used. Human α-thrombin was used over a range of 5–2500 nM.

In the experiments using HD1 and HD22, these oligonucleotides were both used over a concentration range of 0–200 nM. When γ$_T$-thrombin was used, its concentration ranged from 7.8 nM to 1 μM, and HD22 was used at 1 μM.

A progressive increase in the apparent K_d for α-thrombin-GpIb fragment was observed upon HD22 addition. Based on this finding, we analyzed the experimental data by applying a competitive inhibition scheme whereby HD22 competitively inhibits thrombin binding to the immobilized GpIbα fragment and *vice versa*. Such a scheme was previously used to analyze the heparin effect on the thrombin-glycocalicin interaction (8). However, because of its high affinity for thrombin (19), the concentration of free HD22 changes upon binding to thrombin. In this experimental set up, the two interacting macromolecules (thrombin and HD22) were present in comparable amounts. This forced us to use appropriate equations cast in terms of the total, rather than the free, HD22 concentration (20, 21). The latter, Hf, is determined as follows.

$$Hf = (H_t - e_t - K_i + Q)/2 \qquad \text{(Eq. 9)}$$

$$Q - \sqrt{(H_t - e_t - K_i)^2 + 4K_1H_t} \qquad \text{(Eq. 10)}$$

where H_t is the total HD22 concentration, e_t is the total thrombin concentration, and K_i is the equilibrium dissociation constant for thrombin-HD22 interaction. The concentration of bound HD22, Hb, is determined as follows.

$$Hb = H_t - Hf \qquad \text{(Eq. 11)}$$

From a conservation relationship, it is known that the concentration of thrombin bound to HD22, e_b, equals the concentration of bound HD22, Hb. Hence

$$e_f = c_t - Hb \qquad \text{(Eq. 12)}$$

Because of the competitive effect of HD22 on the thrombin-GpIbα interaction, the concentration of thrombin bound to the immobilized GpIbα fragment, $e - \text{GpIb}$, was calculated using the following relation.

$$e - \text{GpIb} = (e - \text{GpIb})_{max} \, cf/(ef + K_d) \qquad \text{(Eq. 13)}$$

where $(e - \text{GpIb})_{max}$ is the maximum value of $e - \text{GpIb}$ complex, and K_d^* (the apparent equilibrium dissociation constant for thrombin-GpIbα interaction in the presence of a given HD22 concentration) is defined by the following equation.

$$K_d^* = K_d^{o}(1 + Hf/K_i) \qquad \text{(Eq. 14)}$$

where K_d^{o} is the true equilibrium dissociation constant for the thrombin-GpIbα interaction and K_i is the HD22-thrombin binding constant.

Experimental points pertaining to the HD22 effect on thrombin-GpIbα were simultaneously fitted to Equations 9–14 to enhance the degrees of freedom in the fitting procedure and provide more robust results (8).

Effect of Intact Platelets on the Heparin-catalyzed Inhibition of Thrombin by Antithrombin III—Platelets, gel filtered as described previously (18), were suspended in 10 mM Hepes, 0.135 M NaCl, 5 mM KCl, 5.5 mM glucose, 2 mM CaCl$_2$ pH 7.4. The platelet suspension (200,000/μl) was divided in two aliquots: one was used as control, and the other one was subjected to mocarhagin treatment (10 μg/ml) at 37 °C for 20 min. At the end of incubation, platelets were centrifuged at 2000 × g for 10 min and washed three times in 10 mM Hepes, 0.15 M NaCl, 0.1% PEG 6000, 10 μM prostaglandin E$_1$, pH 7.40. The final platelet suspensions were treated with 0.4% (final concentration) formaldehyde at 25 °C for 1 h and washed three times in the above buffer. With cytofluorimetric analysis (Becton Dickinson FACScan instrument) using fluorescein isothiocyanate-coupled anti-GpIbα MoAb SZ2, mocarhagin-treated platelets demonstrated minimal labeling compared with control (see below).

The effect of formaldehyde-treated intact or mocarhagin-exposed platelets on the heparin-catalyzed rate of thrombin inhibition by AT was assessed by incubating 0.5–5 nM thrombin at 25 °C with varying concentrations of platelets (30,000–200,000/μl), 15 nM AT, 0.25 μM AT, and 70 μM of the chromogenic substrate Phe-Pip-Arg-pNA in 10 mM Hepes, 0.15 M NaCl, 0.1% PEG 6000, pH 7.50. At intervals, the reaction was stopped by adding 100 nM hirudin, and after precipitating the platelets by centrifugation at 6000 rpm for 5 min, the *p*-nitroaniline in the supernatant was measured at 405 nm. An apparent pseudo-first order rate constant for thrombin inhibition was calculated using GRAFIT software.

Effect of HD1 and HD22 on Thrombin-induced Platelet Aggregation—Platelets, gel filtered as described previously (18), were suspended in 20 mM Hepes, 0.135 M NaCl, 5 mM KCl, 0.2% bovine serum albumin, 5.5 mM glucose, 2 mM CaCl$_2$ pH 7.4. Platelet aggregation in response to 1 nM thrombin was studied using a dual channel aggregometer according to the Born method, in the absence or presence of HD22 or HD1 in concentrations ranging from 1.5 to 400 nM and from 1.5 to 90 nM, respectively. The maximum velocity of absorbance change was measured and expressed as a percentage relative to a control measured in the absence of effector.

Effect of HD22 on Thrombin-induced Calcium Mobilization in Intact and GpIb-depleted Platelets—Intraplatelet calcium mobilization induced by thrombin was evaluated using the fluorescent dye for Ca^{2+}, Fura 2-acetoxymethyl ester, as described previously (18). Fura 2-loaded gel filtered platelets were divided into two aliquots, one of which was subjected to mocarhagin treatment, while the other served as a control. Platelet suspensions were incubated in the presence of 1 mM CaCl$_2$ at 37 °C for 30 min with either 10 μg/ml mocarhagin or buffer alone. At the end of incubation, 2 mM EDTA was added to quench the mocarhagin activity. Intact or mocarhagin-treated platelets were then stimulated
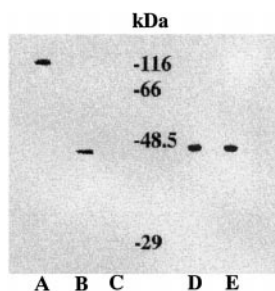
FIG. 1. **SDS-PAGE Western blot under reducing conditions of purified glycocalicin (*A*), purified GpIbα$_{1-282}$ fragment obtained from mocarhagin treatment of washed platelets (*B*), and purified GpIbα$_{1-271}$ fragment obtained from mocarhagin and carboxypeptidase Y treatment (*C*).** The Western blots were accomplished by using the SZ2 MoAb, recognizing the N-terminal region of GpIbα. *D*, SDS-PAGE of purified GpIbα$_{1-282}$; *E*, SDS-PAGE of purified GpIbα$_{1-271}$. In the middle of the figure, the reference molecular mass standards are reported: 116 kDa, β-galactosidase (from *E. coli*); 66 kDa, bovine serum albumin; 48.5 kDa, fumarase (from porcine heart); 29 kDa, carbonic anidrase (from bovine erythrocytes).

with 1 nM α-thrombin in the presence of 25, 100, and 400 nM HD22 aptamer, and the lag time for calcium increase was the parameter used to evaluate the kinetics of calcium increase under the various experimental conditions, as previously detailed (18, 22).

RESULTS

Purification of GpIbα$_{1-282}$ and of GpIbα$_{1-271}$—Mocarhagin treatment of platelets releases a component with a molecular mass of 40 kDa. This purified protein was recognized by a monoclonal antibody, SZ2, directed against the sulfated tyrosine sequence of GpIbα (Fig. 1). In contrast, this monoclonal antibody did not recognize the GpIbα$_{1-271}$, the fragment obtained after 240 min of carboxypeptidase treatment (Fig. 1). After 240-min incubation with immobilized carboxypeptidase Y, the amino acids released from GpIbα$_{1-282}$ were one threonine, one leucine, one proline, two glutamic acid residues, three aspartic acid residues, 2.6 sulfated tyrosine residues, and 0.4 tyrosine residues. This amino acid composition corresponds to the sequence (NH$_2$)DTDLY(S0$_3$)DY(S0$_3$)Y(S0$_3$)PEE(COOH), which is the Asp^{272}–Glu^{282} region of GpIbα. The presence of ~2.6 sulfated tyrosines in the hydrolyzed amino acid mixture is in agreement with previous results suggesting that about 50% of Tyr^{276} is sulfated (9). Although definitive confirmation of the sulfation status of Tyr^{276} is beyond the scope of the present study, it is noteworthy that the peak reflecting the authentic tyrosine (at 41.7 min) was the last to appear during the course of the hydrolysis reaction (data not shown). This suggests that Tyr^{276} may undergo only partial post-translational sulfation.

Effect of Single-stranded DNA Oligonucleotides on α-Thrombin Interaction with GpIbα$_{1-282}$ and GpIbα$_{1-271}$—The effect of HD1 and HD22 on thrombin interaction with immobilized GpIbα$_{1-282}$ and GpIbα$_{1-271}$ was evaluated. HD22 is known to bind with high affinity to thrombin HBS (19). Furthermore, HD22 did not bind to a thrombin variant with mutations in the HBS (Arg^{93} → Ala, Arg^{97} → Ala, and Arg^{101} → Ala; data not shown). These findings confirm the specificity of HD22 for the HBS of thrombin. This aptamer competed with thrombin for GpIbα$_{1-282}$ binding (Fig. 2). Using Equations 9–14 to analyze the data, HD22 binds to α-thrombin with a K_d value of 24 ± 5 nM. This value was in good agreement with the K_d value of 26 nM, determined either by measuring the binding of the aptamer to fluorescently labeled thrombin or the binding of fluorescent aptamer to unlabeled thrombin (data not shown). The K_d value for the thrombin-GpIbα$_{1-282}$ interaction was 149 ± 15 nM, in good agreement with the K_d value of 188 ± 35 nM derived from functional experiments examining the effect of the GpIbα$_{1-282}$
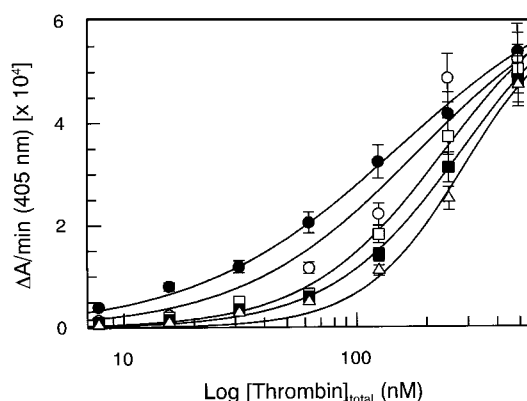

FIG. 2. **Solid phase binding experiments dealing with HD22 effect on thrombin interaction with the immobilized GpIbα$_{1-282}$ fragment.** The total thrombin concentration is reported, and the bound thrombin was evaluated at 0 (●), 50 nM (○), 100 nM (□), 150 nM (■), and 200 nM (△) HD22 oligonucleotide. *Continuous lines* were drawn by simultaneously fitting all the experimental data to Equations 9–14, with the following best fit parameter values: $K_d = 24 ± 5$ nM, and $K_i = 149 ± 15$ nM, and $\Delta A_{max} = 6.96 ± 0.3 × 10^{-4}$ (ΔA/min$_{405\,nm}$). The experimental points are the mean from two different measurements, with the *vertical bars* representing the standard deviations.

fragment on heparin-catalyzed thrombin inhibition by AT, as detailed below.

In contrast, HD1 did not affect α-thrombin binding to GpIbα$_{1-282}$, as shown in Fig. 3. Based on the demonstrated specificity of HD1 interaction with the fibrinogen recognition site on thrombin (23–25), these results rule out a significant contribution of the fibrinogen recognition site to thrombin interaction with GpIbα$_{1-282}$. Using the same solid phase binding assay, immobilized GpIbα$_{1-271}$ did not bind thrombin (Fig. 3), findings consistent with the results obtained in the functional experiments, which demonstrated no effect of the GpIbα$_{1-271}$ fragment on the heparin-catalyzed rate of thrombin inhibition by AT (see below). Altogether, these experiments suggest that the region 272–282 of GpIbα is important in driving the energetics of thrombin interaction.

Interaction of γ$_T$-Thrombin with GpIbα$_{1-282}$—The interaction of γ$_T$-thrombin with immobilized GpIbα$_{1-282}$ is characterized by a K_d value of 281 nM, which is ~85% higher than that of α-thrombin (Fig. 4). Thus, even though γ$_T$-thrombin has an impaired fibrinogen recognition site, it still binds to GpIbα, presumably via its HBS, which is intact (26). HD22 can displace γ$_T$-thrombin from immobilized GpIbα, as shown in Fig. 4. It is noteworthy that in separate experiments HD22 has been shown to bind to γ-thrombin with a K_d value of about 15 nM (data not shown).

Effect of Salt on Thrombin Interaction with the GpIbα$_{1-282}$ Fragment—Measurement of the apparent equilibrium constant of GpIbα$_{1-282}$ fragment binding to α-thrombin, as detailed above, under different salt concentration permits analysis of the electrostatic component of the interaction. Experimental results were analyzed by using the following equation (27, 28).

$$-\ln K_d = A° + \Gamma_± \ln [\text{salt}] \qquad \text{(Eq. 15)}$$

where $A°$ is the value of $-\ln K_d$ where [salt] = 1 M and $\Gamma_±$ is the phenomenological coefficient expressing the linkage between the change in $\ln K_d$ and the change in $\ln$ [salt].

Fig. 5 shows that the plot of the apparent K_d of GpIbα$_{1-282}$ binding to thrombin as a function of salt concentration is linear with $\Gamma_±$ values equal to $-4.6 ± 0.4$ for NaCl and $-4.3 ± 0.4$ for TMACl.

The extrapolated K_d value of GpIbα$_{1-282}$ binding to thrombin at 1 M NaCl and TMACl was equal to $2 ± 0.2$ and $1.6 ± 0.2$ mM,
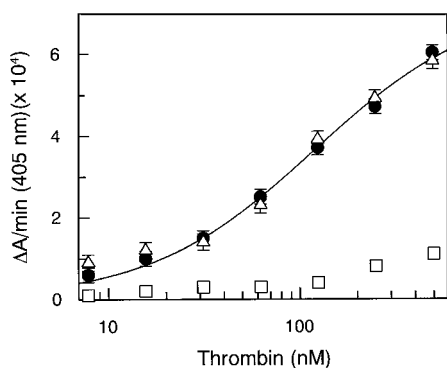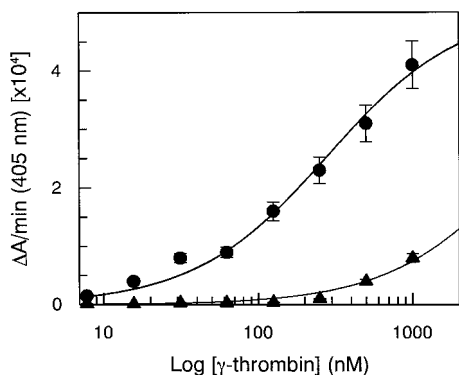
FIG. 3. **Solid phase binding experiments pertaining to thrombin interaction with immobilized GpIbα$_{1-282}$ fragment in the absence (●) and in the presence of 200 nM (△) HD1 oligonucleotide.** The experimental points pertaining to thrombin interaction with immobilized GpIbα$_{1-271}$ (□) are also reported for comparison. The *continuous line*, pertaining to the absence of HD1, was drawn by fitting the experimental points to a single site binding equation with the following best fit parameter values: K_d = 120 ± 11 nM and ΔA_{max} = 7.2 ± 0.3 × 10^{-4} (ΔA/min$_{405\,nm}$).

FIG. 4. **Solid phase binding experiments pertaining to γ$_T$-thrombin interaction with immobilized GpIbα$_{1-282}$ fragment in the absence (●) and in the presence of 1 μM (▲) HD22.** The *continuous line* was drawn by fitting the experimental points to a single site binding equation with the following best fit parameter values: K_d = 281 ± 43 nM and ΔA_{max} = 5.1 ± 0.3 × 10^{-4} (ΔA/min$_{405\,nm}$).
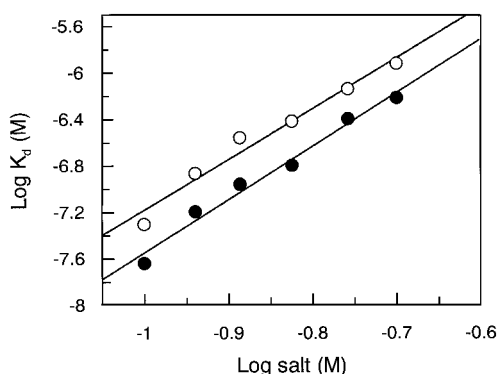

FIG. 5. **Salt dependence of the thrombin interaction with the GpIbα$_{1-282}$ fragment.** The experimental details are reported under "Experimental Procedures." Observed equilibrium dissociation constants (mean of two determinations) of binding to thrombin, K_d, were measured as a function of NaCl (●) and TMACl (○). The linear fits were drawn according to Equation 15, with the following best fit parameter values: $K_d°$ = 2±.2 mM and 1.6 ± 0.2 mM and slope = −4.6 ± 0.4 and −4.3 ± 0.4 for NaCl and TMACl, respectively.

respectively. These values should give the equilibrium dissociation constant reflecting the nonionic driving force for GpIbα binding to thrombin, as previously proposed on the basis of a general thermodynamic analysis (27).
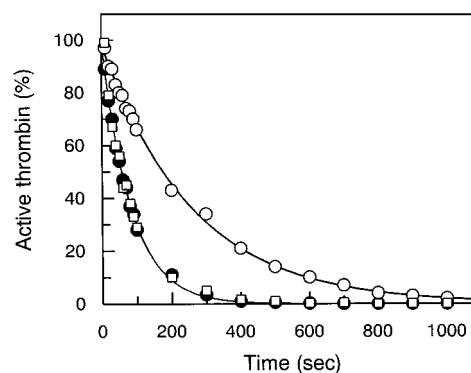

FIG. 6. **Time course of thrombin inactivation by AT-heparin in the absence (●) and presence (○) of 400 nM GpIbα$_{1-282}$ fragment.** Thrombin, AT, and heparin concentrations were equal to 1, 25, and 4 nM, respectively. Experimental points were fitted to Equation 4, with the best fit parameter values of k_{obs} = 1.2 ± 0.02 × 10^{-2} s^{-1} and 3.9 ± 0.08 × 10^{-3} s^{-1} for the reference and the GpIbα$_{1-282}$, respectively. Data points (□) pertaining to the effect of 400 nM GpIbα$_{1-271}$ on thrombin-heparin-AT interaction are also shown.

Finally, it is noteworthy that also the anions present in solution contribute to the electrostatics of thrombin-GpIbα$_{1-282}$ interaction, as at 0.2 M NaF the apparent K_d was 4-fold lower than that measured at 0.2 M NaCl (0.15 μM and 0.6 μM, respectively).

Effect of GpIbα$_{1-282}$ and GpIbα$_{1-271}$ Fragments on Thrombin-AT-Heparin Interaction—GpIbα$_{1-282}$ produced a concentration-dependent decrease in the heparin-catalyzed rate of thrombin inhibition by antithrombin (Figs. 6 and 7). In contrast, GpIbα$_{1-271}$ had no effect on the rate of this interaction (Fig. 6). These findings, together with the binding data, strongly suggest that the region encompassing Asp^{272}–Glu^{282}, which is released by carboxypeptidase Y, contains the thrombin-binding domain.

It is noteworthy that the calculated value of k_{uncat} did not change as a function of GpIbα$_{1-282}$ concentration, as detailed in the legend to Fig. 6, implying that the thrombin-AT interaction *per se* is unaffected by the fragment. Further support for this concept comes from the observation that, in the absence of heparin, the kinetics of the thrombin-AT interaction was unaffected by the GpIbα$_{1-282}$ fragment (k_{inhib} = 8 × 10^3 M^{-1} s^{-1} *versus* 7 × 10^3 M^{-1} s^{-1} in the absence and presence of 1 μM GpIbα$_{1-282}$ fragment, respectively; data not shown).

By applying Equation 6, we analyzed the effect of the GpIbα$_{1-282}$ fragment on the $k_{cat}/K_{T\cdot ATH}$ value of thrombin interaction with the AT-heparin complex. The $k_{cat}/K_{T\cdot ATH}$ value decreased as a function of the GpIbα$_{1-282}$ concentration, consistent with competitive inhibition of thrombin binding to the AT-heparin complex by GpIbα$_{1-282}$. Therefore, the inverse of calculated values of $k_{cat}/K_{T\cdot ATH}$ were fitted to Equation 6 and plotted in Fig. 8. This analysis yielded an apparent K_i value of 188 ± 35 nM at 0.15 M NaCl.

Effect of Intact Platelets on the Heparin-catalyzed Inhibition of Thrombin by Antithrombin III—Paraformaldehyde-treated platelets attenuate the heparin-catalyzed inhibition of thrombin by AT, as shown in Fig. 9. This effect was proportional to the platelet concentration, over a range of 30,000–200,000/μl. Depletion of platelet GpIbα by mocarhagin treatment almost completely eliminated such an effect (Fig. 9). Paraformaldehyde-treated platelets were used in these experiments to circumvent the effect of platelet-derived heparin neutralizing proteins such as platelet factor 4 or von Willebrand factor. Consequently, the inhibiting effect of intact platelets likely reflects GpIbα, which is missing in the mocarhagin-exposed platelets.

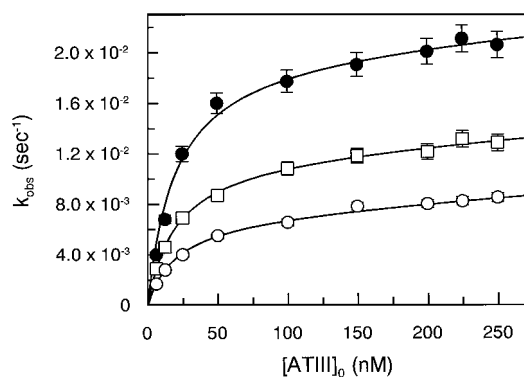The platelet attenuation of the heparin-catalyzed inhibition

FIG. 7. Experimental values of k_{obs} for heparin-catalyzed (4 nM) thrombin inactivation as a function of AT concentration, in the absence (●) and in the presence of 100 nM (□) and 400 nM (○) GpIbα$_{1-282}$. The *continuous lines* were drawn according to Equation 5, with the following best fit parameter values: ●, $k_{cat}/K_{T \cdot ATH} = 2.1 \pm 0.08 \times 10^7$ M^{-1} s^{-1}, $k_{uncat} = 7.3 \times 10^3$ M^{-1} s^{-1}; □, $k_{cat}/K_{T \cdot ATH} = 1.2 \pm 0.1 \times 10^7$ M^{-1} s^{-1}, $k_{uncat} = 7.5 \times 10^3$ M^{-1} s^{-1}; ○, $k_{cat}/K_{T \cdot ATH} = 0.7 \pm 0.03 \times 10^7$ M^{-1} s^{-1}), $k_{uncat} = 7.4 \times 10^3$ M^{-1} s^{-1}.
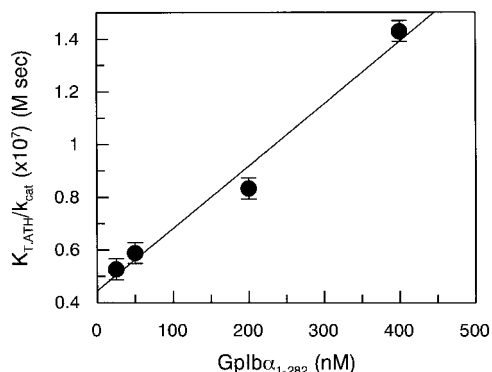

FIG. 8. Dependence of observed values of $K_{T \cdot ATH/k_{cat}}$ on GpIbα$_{1-282}$ concentration, analyzed according to Equation 6 at 0.15 M NaCl. The *continuous line* was drawn according to the above equation with the following best fit parameter values: $K_{T \cdot ATH}/k_{cat}° = 0.44 \pm 0.05 \times 10^{-7}$ M s, $K_i = 188 \pm 35$ nM.
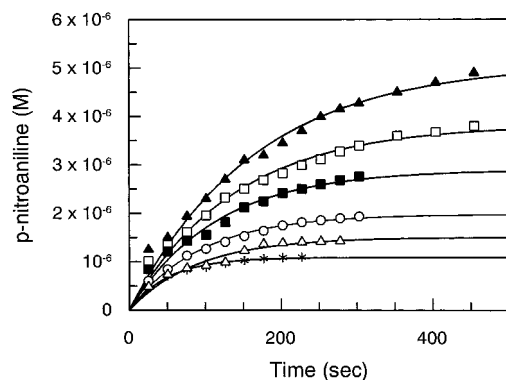

FIG. 9. Effect of paraformaldehyde-treated platelets on the heparin-catalyzed inhibition of thrombin by AT as a function of platelet number. The rate of 70 μM S-2238 hydrolysis by thrombin (0.5 nM) was measured in the presence of 0.25 μM AT and 15 nM heparin. Platelet counts were 0 (*), 30,000/μl (○), 50,000/μl (■), 100,000/μl (□), and 200,000/μl (▲). The heparin-catalyzed inhibition of thrombin by AT was progressively attenuated by increasing platelet counts. GpIb depletion on platelets (200,000/μl) by mocarhagin treatment (△) abolished such an effect.

of thrombin by AT was demonstrated at low thrombin concentration (0.5 nM), whereas at higher enzyme concentration (5 nM), the rate of thrombin inhibition was only minimally affected (data not shown). This phenomenon might reflect the fact that at higher thrombin concentrations, platelets are no
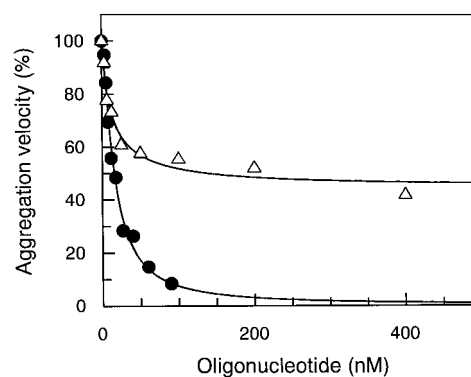

FIG. 10. Effect of HD1 (●) and HD22 (△) on thrombin-induced platelet aggregation. Gel filtered platelets were aggregated by addition of 1 nM human α-thrombin. *Continuous lines* were drawn according to a simple inhibition equation with the best fit IC₅₀ values equal to 15 and 13 nM for HD1 and HD22, respectively.

longer able to buffer all the thrombin molecules present in solution, and a predominant enzyme fraction is free in solution.

Effect of Aptamers on Thrombin-induced Platelet Aggregation—The effect of HD22 and HD1 on thrombin-induced platelet aggregation was investigated to evaluate the contribution of the HBS and FRS domains of thrombin to platelet activation.

Although increasing concentrations of either HD1 or HD22 cause progressive inhibition of thrombin-induced platelet aggregation, there are quantitative differences between the effects of these aptamers. Platelet aggregation was completely abolished at saturating HD1 concentrations (Fig. 10). In contrast, platelet aggregation was markedly inhibited, but not abolished, by HD22. The effect of HD22 is similar to that recently reported for heparin, which also reduced platelet activation in response to thrombin (22). Like heparin, HD22 inhibits thrombin binding to GpIbα, thereby attenuating thrombin-induced platelet aggregation. However, this agent did not abolish aggregation, because it did not prevent thrombin interaction with protease activated receptor(s) on the platelet membrane.

Effect of HD22 on Thrombin-induced Intraplatelet Calcium Mobilization—The HD22 effect on the thrombin-induced calcium mobilization in both intact and in GpIb-depleted platelets was studied to test the hypothesis that a competitive inhibition of the thrombin-GpIb interaction plays a role in the thrombin-induced platelet inhibition observed in aggregation experiments.

After mocarhagin treatment, <10% residual GpIb remained on the platelet membrane (Fig. 11). As previously reported (22), mocarhagin-treated platelets resemble platelets of Bernard-Soulier disease, a congenital deficiency of GpIb, because they exhibit a delayed response to thrombin stimulation resulting in a longer lag time for calcium rise, compared with intact platelets. The MoAb SZ2, which binds to GpIb, exerts the same effect. HD22 has no effect on thrombin-induced calcium mobilization in mocarhagin-exposed platelets. In contrast, HD22 produces a concentration-dependent prolongation of lag time in control platelets (Fig. 12), an effect similar to that of heparin (22). These results suggest that by binding to the thrombin HBS, HD22 inhibits only the GpIb-mediated contribution to platelet activation.

DISCUSSION

Recently, it was found that the major GpIbα fragment, referred to as glycocalicin, reduces the rate of thrombin inactivation by AT by competing with heparin for binding to the HBS on thrombin (8). In the present investigation we tested the hypothesis that the strongly acidic stretch from Asp²⁷² to Glu²⁸² of GpIbα may act as a "heparin-like" ligand for the

FIG. 11. **Histogram analysis of GpIb expression on intact and mocarhagin-treated platelets.** GpIb (CD42b) expression on platelets exposed to mocarhagin is shown on the *left* (*open curve*) and compared with that on intact platelets (*black curve*) on the *right*. Marker was set according to the proper isotypic control. In *parentheses*, geometric mean values of CD42b fluorescence distribution are reported. One of three representative experiments is shown.
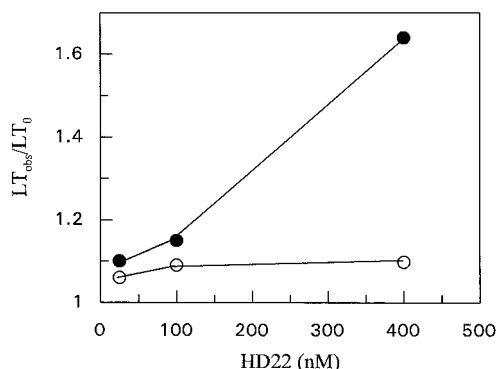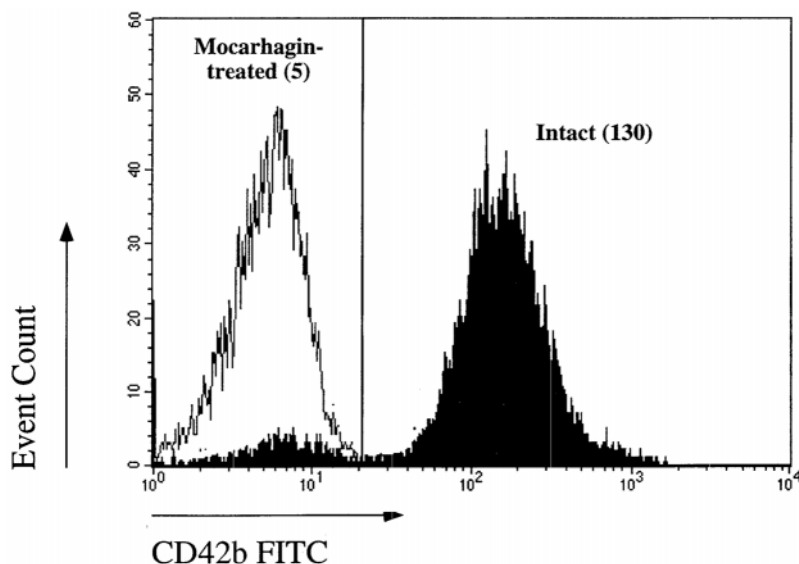

FIG. 12. **Effect of HD22 on α-thrombin-induced calcium increase in intact and mocarhagin-exposed platelets.** The lag time (*LT*) for calcium increase induced by 1 nM α-thrombin was measured in intact (●) and mocarhagin-treated (○) platelets as a function of HD22 concentration. For both platelet preparations, the value obtained at each HD22 concentration was divided by the respective control value (LT_o) obtained in the presence of buffer alone.

thrombin HBS, being thus responsible for the competitive inhibition of heparin interaction with thrombin. The data reported in this study show that GpIbα$_{1–282}$ reduces the rate of the heparin-catalyzed thrombin inhibition by AT. This finding is in agreement with previous data indicating that the region of the GpIbα molecule involved in thrombin ligation encompasses a large domain of the glycoprotein spanning from Cys²⁰⁹ to Asp²⁸⁷ (6, 29–32). This region bears a peculiar stretch of acidic residues from Asp²⁶⁹ to Asp²⁸⁷ comprising three sulfated groups linked to Tyr²⁷⁶, Tyr²⁷⁸, and Tyr²⁷⁹ (9, 29–32). In this study we present evidence suggesting that the Asp²⁷²–Glu²⁸² region is an essential part of the thrombin-binding domain. This result emerged from both solid phase binding experiments and functional studies that investigated the effect of different GpIbα fragments on the heparin-catalyzed thrombin inhibition by AT. In particular, the salt dependence of GpIbα$_{1–282}$ binding to thrombin confirmed the major role played by ionic interactions in the formation of the thrombin-GpIbα adduct. These studies showed an invariance of the $\Gamma_\pm$ value in NaCl and TMACl. This suggests that the parameter is actually an index of the electrostatic screening of ions on the surface of the interacting proteins. It is of interest that the same parameter value for binding of heparin to thrombin is equal to −4.8 (33). On the other hand, binding of the hirudin fragment 55–65 to the fibrinogen recognition site of the enzyme, has $\Gamma_\pm$ values of

−1.06 and −1.35 in NaCl and choline chloride, respectively (33, 34). Thus, the present results, together with the previous findings, reasonably exclude an involvement of the fibrinogen recognition site of thrombin and provides further support for the concept that the HBS mediates the interaction of thrombin with GpIbα$_{1–282}$. The relevance of thrombin HBS in GpIbα ligation was previously demonstrated by our group in experiments using thrombin chemically modified with pyridoxal phosphate at HBS domain (7, 22). These experiments showed that HBS-modified thrombin exhibited both decreased binding to GpIbα and reduced platelet activating capacity (7, 22). The HBS domain may act as a polyelectrolyte-like segment that is able to make multiple salt bridges with the polyanionic segment Asp²⁷²–Glu²⁸² on the GpIbα molecule.

Recent thermodynamic data showed the occurrence of heat capacity change (expression of a hydrophobic effect, equal to −1 kcal/mol) in the thrombin-glycocalicin interaction (8). The current results may be reconciled with the above finding by hypothesizing that the numerous salt bridges between the two proteins occur along with burial of a large number of solvating water molecules when thrombin binds to GpIbα, as this solvation process is characterized by a negative heat capacity change (35).

The above findings strongly suggest that GpIbα$_{1–282}$, and particularly the segment from Asp²⁷² to Glu²⁸², binds to the thrombin HBS. The heparin-binding site resides at the C terminus of the B-chain of thrombin and is mainly formed by a cluster of cationic residues such as Arg⁹³, Arg⁹⁷, Arg¹⁰¹, Arg¹⁷⁵, Arg²³³, Lys²³⁶, and Lys²⁴⁰ (36–39).[2] Our observation that the $\Gamma_\pm$ parameter is very similar to that pertaining to thrombin interaction with heparin raises the possibility that the same cationic residues in the thrombin molecule mediate both interactions. Recent studies with thrombin variants support this concept. Two thrombin variants with mutations in the HBS (Arg⁹³ → Glu and Lys²³⁶ → Glu) did not bind to GpIbα. In contrast, a thrombin variant with a mutation in the FRS (Arg⁹³ → Glu) bound GpIb with an affinity similar to that of native enzyme (40). These results are in agreement with our finding that γ$_T$-thrombin, characterized by a severe modification of FRS and by a normal HBS (26), can bind to GpIbα, although with an affinity that is about 2-fold lower than that of α-thrombin. This may be due to a perturbation in γ$_T$-thrombin of the

---

[2] The thrombin residue numbers used in the text correspond to residue numbers in the chymotrypsin numbering system.

allosteric linkage between FRS and HBS, recently described for human α-thrombin (41).

Further support for the concept that GpIbα interacts with the thrombin HBS comes from experiments using HD1 and HD22. Only HD22, which specifically binds to HBS on thrombin (19), displaced thrombin from immobilized GpIbα$_{1–282}$. In contrast, HD1, which binds to FRS on thrombin (23–25), had no effect.

Another ligand for thrombin HBS, the kringle prothrombin fragment 2, has been recently shown to competitively inhibit the binding of glycocalicin to thrombin (8). Fragment 2 also bears a peculiar anionic motif, DGDEE (residues 68–72), that makes electrostatic interactions with some residues of the thrombin HBS, such as Arg^{93}, Arg^{97}, Arg^{101}, and Arg^{175} (42, 43).

A recent study by Dr. Guillin's group (44) showed that glycocalicin reduces the rate of heparin-catalyzed inhibition of both thrombin and Factor Xa by AT. These investigators claimed that this effect arises from glycocalicin interaction with heparin, rendering less heparin available to activate AT (44). However, this interpretation is not compatible with our data, suggesting that the highly acidic GpIbα stretch 272–282 must be present for GpIbα to compete with heparin for binding to the HBS on thrombin. It is unlikely that this region is able to interact with heparin because of its high content of acidic residues. Moreover, analysis of the GpIbα sequence 1–450 did not show any region bearing a "consensus sequence" (such as COOH-*XXX*-R-*XXX*-RR-*XX*-RR-*XXX*-R-NH$_2$) that appears necessary for a specific interaction with heparin (45, 46). Further support for this comes from the work of other investigators who have shown that heparin blocks the von Willebrand factor-GpIbα interaction by binding to the heparin-binding site of von Willebrand factor and not by binding to GpIb (47). It may be thus hypothesized that the high electrostatic component of thrombin-GpIbα interaction involving the thrombin HBS and the Asp^{272}–Glu^{282} region of GpIb may act to correctly orient the two macromolecules, reducing the free energy necessary for the molecular recognition.

The platelet aggregation experiments demonstrated that thrombin binding to GpIb might exert a positive effect on platelet activation, because HD-22 could attenuate, although not abolish, the aggregation by thrombin. The effect of HD22 on thrombin-induced platelet activation may be explained by its inhibition of thrombin's HBS ligation to GpIbα, as demonstrated by binding experiments. Moreover, HD-22 could not exert its inhibitory activity on platelets depleted of GpIb, as demonstrated by calcium mobilization experiments. This phenomenon was similarly demonstrated for heparin (22). The incomplete inhibition of platelet activation observed with HD-22 and heparin is in agreement with other conditions in which the thrombin-GpIb interaction is inhibited. In fact, Bernard-Soulier or mocarhagin-treated platelets lacking GpIb show a reduced but not abolished response to thrombin. On the contrary, blockage of thrombin FRS by HD-1 could cause a complete inhibition of platelet activation, because the binding of the enzyme to protease-activated receptor(s) molecules and, as a consequence, their hydrolysis was inhibited by the aptamer. Altogether these results corroborate the hypothesis that GpIb does not bind to the thrombin FRS.

How GpIb can contribute to platelet activation by thrombin is not yet clear. One possible mechanism is that thrombin ligation to GpIb may modulate the expression and/or the hydrolysis of protease-activated receptor-1 and protease-activated receptor-4 molecules on the platelet membrane (19, 48–51). This hypothesis deserves further study.

The physiological role of GpIbα binding to the thrombin HBS remains to be elucidated. The results obtained *in vitro* showed that at thrombin concentrations <5 nM, the enzyme binding to the high affinity GpIb site protects it from the heparin-catalyzed inhibition by AT. This phenomenon may represent a general mechanism by which low thrombin concentrations, being protected from inactivation, may enhance the availability of catalytically active thrombin necessary for procoagulant activities, such as platelet activation or conversion of fibrinogen to fibrin. These processes involve the active site and the FRS on thrombin, domains not involved in GpIb ligation. If this mechanism occurs *in vivo*, then the thrombin-GpIb interaction may serve to regulate thrombin activity.

REFERENCES

1. Clemetson, K., and Clemetson, J. (1995) *Semin. Thromb. Haemostasis* **21,** 130–137
2. Buchanan, S. S. C., and Gay, N. J. (1996) *Prog. Biophys. Mol. Biol.* **65,** 1–44
3. Greco, N. J., Tandon, N. N., Jones, G. D., Kornhauser, R., Jackson, B., Yamamoto, N., Tanoue, K., and Jamieson, G. A. (1996) *Biochemistry* **35,** 906–914
4. Greco, N. J., Jones, G. D., Tandon, N. N., Kornhauser, R., Jackson, B., and Jamieson, G. A. (1996) *Biochemistry* **35,** 915–921
5. Lopez, J. A. (1997) *Blood Coagul. Fibrinolysis* **5,** 97–119
6. Gralnick, J. R., Williams, L. P., McKeown, K., Hansmann, J. W., Fenton, J. W., and Krutzsch, H. (1994) *Proc. Natl. Acad. Sci. U. S. A.* **91,** 6334–6338
7. De Candia, E., De Cristofaro, R., De Marco, L., Mazzucato, M., Picozzi, M., and Landolfi, R. (1997) *Thromb. Haemostasis* **77,** 735–740
8. De Cristofaro, R., De Candia, E., Croce, G., Morosetti, R., and Landolfi, R. (1998) *Biochem. J.* **332,** 643–650
9. Ward, C. M., Andrews, R. K., Smith, A. I., and Berndt, M. C. (1996) *Biochemistry* **35,** 4929–4938
10. De Cristofaro, R., Rocca, B., Bizzi, B., and Landolfi, R. (1993) *Biochem. J.* **289,** 475–480
11. Nordenman, B., and Björk, I. (1978) *Biochemistry* 3339–3344
12. Nordenman, B., Nyström, G., and Björk, I. (1977) *Eur. J. Biochem.* **78,** 195–203
13. Lopez, J. A., Chung, D. W., Fujikawa, K., Hagen, F. S., Papayannopoulou, T., and Roth G. J. (1987) *Proc. Natl. Acad. Sci. U. S. A.* **84,** 5615–5619
14. Pace, C. N., Vajdos, F., Fee, L., Grimsley, G., and Gray, T. (1995) *Protein Sci.* **4,** 2411–2423
15. Levina, N. B., and Nazimov, I. V. (1984) *J. Chromatogr.* **286,** 207–216
16. Olson, S. T., and Björk, I. (1991) *J. Biol. Chem.* **266,** 6353–6364
17. Olson, S. T., Björk, I., and Shore, J. (1993) *Methods Enzymol.* **222,** 525–559
18. De Cristofaro, R., De Candia, E., Picozzi, M., and Landolfi, R. (1995) *J. Mol. Biol.* **245,** 447–458
19. Tasset, D. M., Kubik, M. F., and Steiner, W. (1997) *J. Mol. Biol.* **272,** 688–698
20. Cha, S. (1975) *Biochem. Pharmacol.* **24,** 2177–2185
21. Cha, S. (1976) *Biochem. Pharmacol.* **25,** 2695–2702
22. De Candia, E., De Cristofaro, R., and Landolfi, R. (1999) *Circulation* **99,** 3308–3314
23. Bock, L. C., Grifin, L. C., Latham, J. A., Vermass, E. H., and Toole, J. J. (1992) *Nature* **355,** 564–566
24. Wu, Q., Tsiang, M., and Sadler, J. E. (1992) *J. Biol. Chem.* **267,** 24408–24412
25. Padmanabhan, K., Padmanabhan, K. P., Ferrara, J. D., Sadler, J. E., and Tulinsky, A. (1993) *J. Biol. Chem.* **268,** 17651–17654
26. Rydel, T. J., Yin, M., Padmanabhan, K. P., Blankenship, D. T., Cardin, A. D., Correa, P. E., Fenton, J. W., II, and Tulinsky, A. (1994) *J. Biol. Chem.* **269,** 22000–22006
27. Record, M. T., Jr., Anderson, C. F., and Lohman, T. M. (1978) *Q. Rev. Biophys.* **11,** 103–108
28. Record, M. T., Jr., and Anderson, C. F. (1995) *Biophys. J.* **68,** 786–794
29. Marchese, P., Murata, M., Mazzucato, M., Pradella, P., De Marco, L., and Ruggeri, Z. M. (1995) *J. Biol. Chem.* **270,** 9571–9578
30. Hess, D., Schaller, J., Rickli, E. E., and Clemetson, K. J. (1991) *Eur. J. Biochem.* **199,** 389–393
31. De Marco, L., Mazzucato, M., Masotti, A., and Ruggeri, Z. M. (1994) *J. Biol. Chem.* **269,** 6478–6484
32. Dong, J. F, Li, C. Q., and Lopez, J. A. (1994) *Biochemistry* **33,** 13946–13953
33. Olson, S. T., Halvorson, H. R., and Björk, I. (1991) *J. Biol. Chem.* **266,** 6342–6352
34. Vindigni, A., White, C. E., Komives, E. A., and Di Cera, E. (1997) *Biochemistry* **36,** 6674–6681
35. Edsall, J. T., and Wyman, J. (1958) in *Biophysical Chemistry*, pp. 151–162, Academic Press, New York
36. Gan, Z. R., Li, Y., Chen, Z., Lewis, S. D., and Shafer, J. A. (1994) *J. Biol. Chem.* **269,** 1301–1305
37. He, X., Ye, J., Esmon, C. T., and Rezaie, A. R. (1997) *Biochemistry* **36,** 8969–8976
38. Sheean, J. P., and Sadler, J. E. (1994) *Proc. Natl. Acad. Sci. U. S. A.* **91,**

5518–5522

39. Bode, W., Turk, D., and Karshikov, A. (1992) *Protein Sci.* **1,** 426–471
40. Li, C. Q., Vindigni, A., Di Cera, E., Sadler, J. E., and Wardell, M. R. (1997) *Blood* **90**, (Suppl. 1), 430–431 (abstr.)
41. Fredenburgh, J. C., Stafford, A. R., and Weitz, J. I. (1997) *J. Biol. Chem.* **272,** 25493–25499
42. Arni, R. K., Padmanabhan, K., Padmanabhan, K. P., Wu, T. P., and Tulinsky, A. (1993) *Biochemistry* **32,** 4727–4737
43. Liaw, P. C. Y., Fredenburgh, J. C., Stafford, A. R., Tulinsky, A., Austin, R. C., and Weitz, J. I. (1998) *J. Biol. Chem.* **273,** 8932–8939
44. Jandrot-Perrus, M., Clemetson, K. J., Guillin, M. C., and Bouton, M. C. (1999) *Thromb. Haemostasis* **81,** 316–317

45. Cardin, A. D., and Weintraub, H. J. R. (1989) *Atherosclerosis* **9,** 21–32
46. Margalit, H., Fischer, N., and Ben-Sasson, S. A. (1993) *J. Biol. Chem.* **268,** 19228–19231
47. Sobel, M., McNeill, P. M., Carlson, P. L., Kermode, J. C., Adelman, B., Conroy, R., and Marques, D. (1991) *J. Clin. Invest.* **87,** 1787–1793
48. Vu, T. K., Wheaton, V., and Coughlin, S. R (1991) *Cell* **64,** 1057–1068
49. Connolly, A. J., Ishihara, H., Kahn, M. L., Farese, R. V., Jr., and Coughlin, S. R (1996) *Nature* **381,** 516–519
50. Ishihara, H., Connolly, A. J., Zeng, D., Kahn, M. L., Zheng, Y. W., Timmons, C., Tram, T., and Coughlin, S. R. (1997) *Nature* **386,** 502–506
51. Kahn, M. L., Nakanishi-Matsui, M., Shapiro, M. J., Ishihara, H., and Coughlin, S. R. (1999) *J. Clin. Invest.* **103,** 879–887

The Asp^{272}–Glu^{282} Region of Platelet Glycoprotein Ibα Interacts with the Heparin-binding Site of α-Thrombin and Protects the Enzyme from the Heparin-catalyzed Inhibition by Antithrombin III

Raimondo De Cristofaro, Erica De Candia, Sergio Rutella and Jeffrey I. Weitz